

1 **ThX – A next-generation probe for the early detection of amyloid aggregates**

2

3 Lisa-Maria Needham^{\$a}, Judith Weber^{\$a,b,c}, Juan A. Varela^a, James W. B. Fyfe^d, Dung T. Do^d,
4 Catherine K Xu^a, Benjamin Keenlyside^a, Rachel Cliffe^a, David Klenerman^a, Christopher M.
5 Dobson^a, Christopher A. Hunter^a, Sarah E. Bohndiek^{b,c}, Thomas N. Snaddon^{d*}, and Steven F.
6 Lee^{a*}.

7 * - denotes joint corresponding authors

8 \$ - denotes equal contributions

9

10 **Author Affiliations**

11 ^a Department of Chemistry, University of Cambridge, Cambridge, CB2 1EW, U.K.

12 ^b Department of Physics, University of Cambridge, Cambridge, CB3 0HE, U.K.

13 ^c Cancer Research UK Cambridge Institute, University of Cambridge, Cambridge, CB2 0RE,
14 U.K.

15 ^d Department of Chemistry, University of Indiana Bloomington, Indiana, 47405-7102, U.S.A.

16

17 **Abstract**

18 Neurodegenerative diseases such as Alzheimer's and Parkinson's are associated with protein
19 misfolding and aggregation. Recent studies suggest that the small, rare and heterogeneous
20 oligomeric species, formed early on in the aggregation process, may be a source of
21 cytotoxicity. Thioflavin T (ThT) is currently the gold-standard fluorescent probe for the study
22 of amyloid proteins and aggregation processes. However, the poor photophysical and binding
23 properties of ThT impairs the study of oligomers. To overcome this challenge, we have
24 designed Thioflavin X, (ThX), a next-generation fluorescent probe which displays superior
25 properties; including a 5-fold increase in brightness and 7-fold increase in binding affinity to
26 amyloidogenic proteins. As an extrinsic dye, this can be used to study unique structural
27 amyloid features both in bulk and on a single-aggregate level. Furthermore, ThX can be used
28 as a super-resolution imaging probe in single-molecule localisation microscopy. Finally, we
29 demonstrate that ThX can be used to detect a distinct oligomeric species, not observed via
30 traditional ThT imaging.

31

32 **Introduction**

33 The study of protein misfolding and aggregation is crucial for understanding the molecular
34 mechanisms that underpin neurodegenerative diseases, such as Parkinson's and
35 Alzheimer's. These neurological disorders share the hallmark of converting soluble proteins
36 into amyloid deposits, which are characterized by a common cross- β core structural motif (Fig.
37 1A)¹. Several recent studies have suggested that the small soluble oligomeric intermediates,

38 which arise during the fibril formation process, are strongly implicated in cytotoxicity and
39 ultimately neuronal cell death². These potentially toxic oligomers are highly heterogeneous in
40 their size and structure, and are rare in abundance (<1%) relative to the monomeric protein³.
41 This renders them challenging to identify and characterize with ensemble biophysical
42 techniques, thus there is currently a lack of suitable tools and methods to study these
43 potentially pathogenic oligomeric species and their formation processes.

44

45 The availability of improved optical probes that allow single-aggregate visualization may
46 provide a potential solution to this problem. One of the main tools for studying amyloid fibril
47 formation is Thioflavin T (ThT), a benzothiazole salt and molecular-rotor dye⁴, which has been
48 used extensively as the 'gold-standard' in the aggregation field due to its amyloid-binding
49 properties⁵⁻¹⁴. Upon binding to β -sheet-rich structures, the fluorescence intensity of ThT
50 increases by several orders of magnitude, making it a sensitive and efficient reporter of
51 amyloid¹⁵. Additionally, new microscopy techniques couple the photophysical properties of
52 ThT with single-molecule instrumentation enabling direct observation of aggregates at
53 diffraction-limited resolution both *in vitro*^{16,17} and in human biofluids^{18,19}. Nevertheless, the low
54 molar extinction coefficient, average quantum yield and low binding affinity of ThT mean it is
55 poorly suited to detection of smaller oligomeric species, particularly in biological samples.
56 Therefore, there remains an unmet need for new fluorescent probes with improved
57 photophysical and binding properties to detect and characterize the formation of these early
58 oligomeric species and their role in the pathogenesis of neurodegenerative disorders.

59

60 To address this, we have designed a novel ThT derivative, ThX, that outperforms ThT in its
61 binding and optical characteristics but still retains the fluorescence enhancement attained
62 upon binding to β -sheet containing species. To achieve this, we increased electron density on
63 the benzothiazole core ring by exchanging the appended methyl group for the corresponding
64 methoxy moiety, and we embedded the dimethyl amino moiety within a pyrrolidine in order to
65 restrict rotation around the C(sp³)-N σ -bonds (Fig. 1A). This resulted in a more electron-rich,
66 more conformationally restricted benzothiazole salt with increased lipophilicity. These
67 properties improved the brightness ($\epsilon \times \Phi_{Fl}$ or integrated fluorescence intensity) upon binding
68 to recombinant, wild-type α -Synuclein (α Syn) aggregates by 5-fold and increased the binding
69 affinity by 7-fold. This resulted in enhanced detection of early α Syn oligomeric species with
70 higher sensitivity both in bulk as well as at the single-aggregate level. In addition, we were
71 able to exploit the transient nature of ThX binding to α Syn aggregates and demonstrate its
72 excellent super-resolution imaging capabilities.

73

74

75 Results and Discussion

76 Initially, to characterize ThX in bulk, the emission properties of the dye were assessed in
 77 aqueous solution in the absence of α Syn aggregates. ThT behaves as a molecular rotor in
 78 low viscosity environments, undergoing rapid rotation around the carbon-carbon σ -bond
 79 between the dimethylaniline and benzothiazole rings²⁰. Therefore, photoexcitation induces the
 80 formation of a twisted intramolecular charge transfer (TICT) state and a low observed
 81 fluorescence quantum yield (Φ_{F1}). In high viscosity environments this rotation is more restricted
 82 resulting in an increase in Φ_{F1} . ThX exhibited viscosity dependent fluorescence intensity
 83 characteristic of ThT, which suggests that ThX also behaves as a molecular rotor (Fig. 1B).
 84 ThT is believed to bind transiently along the side chain channels that make up the β -sheet
 85 architecture of amyloids²¹ during which it is conformationally restricted (Fig. 1A).
 86 Consequently, binding induces a large increase in Φ_{F1} .

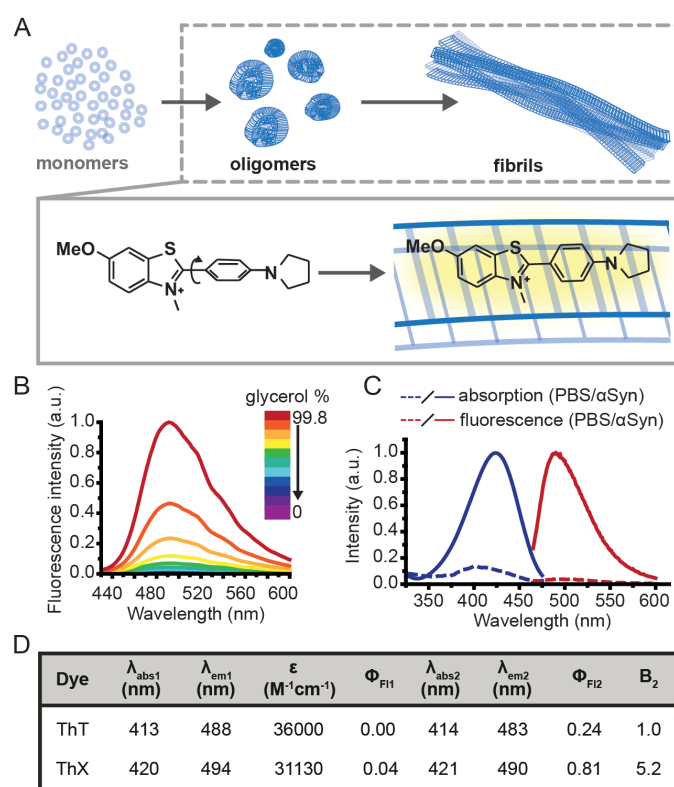


Fig. 1. A) Schematic illustration of the nucleated pathway of amyloid fibril formation starting from monomeric proteins and the common cross- β sheet motif of amyloid fibrils to which benzothiazole salts bind transiently along the long fibril axis. The binding of ThX to the fibrils restricts the rotation around the carbon-carbon bond resulting in a fluorescence turn-on response. **B)** Fluorescence spectra of ThX in increasing glycerol concentration, showing the viscosity dependence of emission properties of the molecular rotor dye. **C)** Absorption and fluorescence spectra of ThX free in PBS and bound to α Syn aggregates. **D)** Table of bulk photophysical properties of ThX and ThT including; maximum absorption wavelength in PBS (λ_{abs1}) and with α Syn aggregates (λ_{abs2}), maximum emission wavelength in PBS (λ_{em1}) and with α Syn aggregates (λ_{em2}), molar extinction coefficient (ϵ), fluorescence quantum yield in PBS (Φ_{F1}) and with α Syn aggregates (Φ_{F2}) and the relative brightness (integrated fluorescence intensity) with α Syn aggregates normalized to ThT (B_2).

87

88 ThX also demonstrated a characteristic increase in Φ_{FI} upon binding to α Syn aggregates in a
 89 similar manner to ThT, as a result of reduced C-C bond torsion (Fig. 1C, D, Fig. S1) However,
 90 the Φ_{FI} of ThX in the presence of α Syn ($\Phi_{FI2} = 0.81$) was ~ 3.4 times larger than ThT ($\Phi_{FI2} =$
 91 0.24) and its brightness (defined as the total integrated emission intensity) outperformed ThT
 92 by $>500\%$. The emission properties of ThX are a convolution of both the intrinsic photophysics
 93 and the affinity with which it binds to amyloid aggregates. Therefore, the capabilities of ThX
 94 and ThT to bind α Syn aggregates were compared. The binding affinities were obtained with
 95 direct fluorescence titrations yielding K_d values of $4.8 \pm 1.3 \mu\text{M}$ for ThT and $0.68 \pm 0.1 \mu\text{M}$ for
 96 ThX, a $>700\%$ improvement in α Syn affinity (Fig. 2Ai). This significantly increased binding
 97 affinity was mirrored at the single aggregate level and allowed ThX SAVE imaging at 3 orders
 98 of magnitude lower concentration compared to ThT, with ThX clearly obtaining high quality
 99 images of α Syn aggregates at concentrations as low as 500 pM (Fig. 2Aii, Fig. S2).

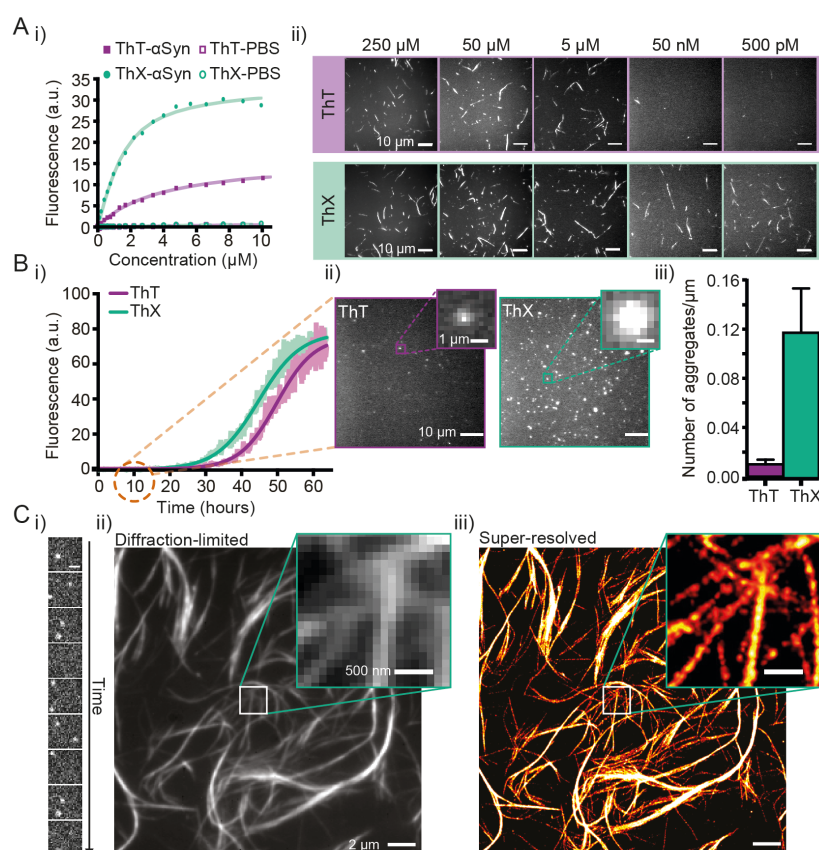


Fig. 2. A) i) Representative binding curves of ThX and ThT binding to α Syn aggregates obtained by direct fluorescence titrations in the presence of 2 μM α Syn. ii) Single-aggregate fluorescence images of α Syn fibrils with ThT (top) or ThX (bottom) at concentrations between 250 μM - 500 pM. **B)** i) Kinetics of α Syn amyloid fibril formation monitored by ThX and ThT. The solid lines indicate the fitted sigmoidal growth curve, the brighter shadows the averaged values obtained from a minimum N=7 independent α Syn aggregations. ii) Fluorescence images taken with 5 μM ThT (left) and ThX (right) of single α Syn aggregates formed 10 hours into the aggregation. The insets show a representative single aggregate. iii) A bar graph showing the density of single 10-hour α Syn aggregates detected with ThT and ThX. Error bars represent standard deviations from 27 fields of view. **C)** i) Time montage showing single ThX molecules transiently binding to a region of an α Syn fibril (scale bar = 500 nm.) ii) Diffraction limited and ii) super-resolved image of α Syn fibrils. Detailed structural features are obscured in the diffraction limited image which can only be seen once the image has been super-resolved (insets).

100

101 Next, we explored whether ThX can be used to monitor the process of amyloid formation
102 through protein aggregation. First, using ThT and ThX, bulk kinetic measurements of
103 recombinant α Syn protein aggregations were performed in parallel. The formation of α Syn
104 fibrils followed the expected sigmoidal growth curves, consistent with multiple previous
105 studies^{12,14,22}(Fig. 2Bi). A clear signal with an intensity of 5% above the baseline signal, was
106 reached at 26.3 ± 1.4 hours for ThX and 34.1 ± 0.8 hours for ThT (Fig. S3). These data
107 indicated that ThX was able to detect aggregate formation at significantly earlier times than
108 ThT in the bulk. This was further confirmed at the single aggregate level with ThX detecting
109 7.5-fold more species than ThT 10 hours into the aggregation (Fig. 2Bii). The differences were
110 not caused by different abilities of ThX and ThT to inhibit the aggregation process (Fig. S4).
111 In addition, ThX a generic probe and also outperforms ThT in its detection capabilities with
112 other amyloid proteins such as amyloid- β peptide ($A\beta_{1-42}$) and P301S tau at both the bulk (Fig.
113 S5) and single aggregate level (Fig. S6).

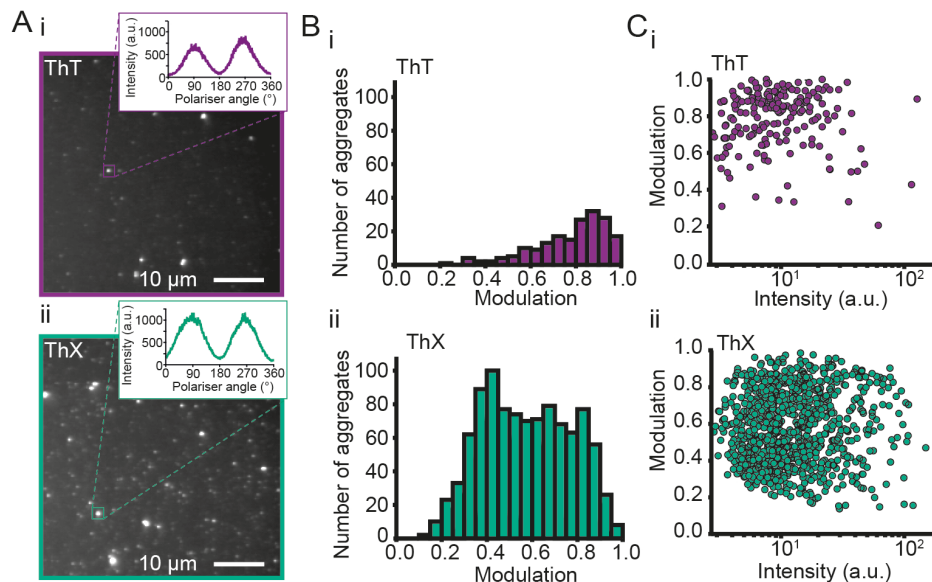


Fig. 3. A) Representative fluorescence anisotropy images of α Syn aggregates 6 hours into the aggregation reaction with i) ThT and ii) ThX. **B)** Histograms of the extent of modulation of single α Syn aggregates detected with i) ThT and ii) ThX. **C)** Relationship between extent of modulation of α Syn aggregates and i) ThT or ii) ThX mean fluorescence intensity measured during the rotation of the polariser minus the background intensity. For each dye, N=3 separate aggregation reactions were tested, and slides were imaged at minimum three different fields of view.

114 Although ThX demonstrated superior photophysical and binding properties in the bulk and
115 single-aggregate detection regimes, smaller spatial information, (i.e. oligomeric species) are
116 still obscured by the diffraction limit (~ 250 nm). Spehar and Lew *et al.* previously demonstrated
117 the use of ThT as a super-resolution probe by exploiting the transient nature of its binding to
118 amyloid proteins and its low solution Φ_{FI} in a method termed transient amyloid binding (TAB)²³

119 Interestingly, ThX obeys similar principles; by excitation with 488 nm light and collection at
120 ~587 nm, one can generate isolated fluorescent puncta of single ThX molecules (Fig 2Ci,
121 Supplementary movie 1). These localisations can be summed to generate diffraction-limited
122 images of α Syn fibrils (Fig. 2Cii) as well as fit and reconstructed to produce super-resolved
123 images (Fig. 2Ciii) of α Syn fibrils, achieving a mean localisation precision of 21.0 nm (Fig.
124 S7A) and an image resolution of 18.3 nm (Fig. S7B), determined by Fourier ring correlation
125 analysis²⁴.

126
127 Amyloid aggregates are diverse in size, structure and formation mechanism. Previous work
128 has provided evidence for a structural rearrangement from disordered aggregates to ordered
129 fibrils during the aggregation process^{19,25,26}. We have previously developed an all-optical
130 method to characterize the structural order of individual protein aggregates by measuring the
131 fluorescence anisotropy of bound ThT¹⁹. We employed this technique to elucidate whether
132 ThX was sensitive to alternative binding modes in both α Syn fibrils and oligomers. For both
133 ThX and ThT the fluorescence intensity modulated sinusoidally in the same phase when
134 bound to ordered structures (Fig. S8), suggesting that the two dyes are oriented the same way
135 in this circumstance. However, when applied to early α Syn aggregates (6-hour time point, Fig.
136 3A) ThX could observe large numbers of both modulating (>0.5 , β -sheet 'ordered') and non-
137 modulating (<0.5 , β -sheet 'disordered') distributions (Fig. 3Bii). This disordered aggregate
138 population was not detected when using ThT alone (Fig. 3Bi). Photon-fluence matched
139 experiments confirmed that both species (albeit fewer in number) could be observed with ThX
140 but not ThT (Fig. S9) and that this was not just a product of the increased affinity. Furthermore,
141 the degree of modulation was not correlated to the fluorescence intensity (Fig. 3Ci-ii, Fig S10).
142 This may suggest that the number of binding sites remains unchanged during the structural
143 rearrangement of the aggregates, and that the ability of ThX to detect different species is not
144 just a result of the increased brightness of ThX. In combination, these data support the notion
145 that ThX is able to detect a structurally distinct oligomeric species. We expect that the
146 capabilities of this new probe will be of broad interest to the aggregation community.

147

148 **Conclusions**

149 We have designed and evaluated ThX, a novel ThT derivative with improved photophysical
150 and binding properties that may prove superior to ThT in future applications. ThX can detect
151 β -sheet species at early time points in the aggregation of amyloid proteins at both the bulk
152 and single-aggregate levels, as well as additional structurally distinct species that are not
153 observed with ThT. In addition, ThX is compatible with super-resolution imaging and capable
154 of resolving nano-scale structural features with ~20 nm precision. Taken together, ThX may
155 allow the study of the formation of earlier pathological amyloid species and exploration of their

156 role in the pathogenesis of neurodegenerative disorders. Furthermore, the unique properties
157 of ThX might enable the study of these amyloids in high background biological samples such
158 as cerebrospinal fluid and blood plasma.

159

160 **Contributions**

161 J.W., L.M.N., S.F.L. and T.N.S. designed the experiments, T.N.S., J.W.B.F. and D.T.D.
162 synthesized the molecules. J.W. and L.M.N. performed bulk fluorescence characterisation
163 measurements and analyses. J.W. prepared the α Syn aggregates, performed bulk protein
164 binding assays and aggregation time-course experiments. J.W. and C.A.H. analysed binding
165 data. L.M.N. performed the single-aggregate fluorescence imaging, super-resolution imaging
166 and analyses. J.W. and J.A.V. performed fluorescence polarisation experiments. J.A.V.
167 analysed fluorescence polarisation data. J.W., L.M.N., S.F.L. and T.N.S. wrote the manuscript.

168

169 **Acknowledgements**

170 We thank the Royal Society for the University Research Fellowship of S.F.L. (UF120277). This
171 work was funded in part by the Michael J Fox Foundation and The University of Indiana. We
172 thank the EPSRC for the Doctoral Prize of L.M.N. J.W, and S.E.B. are funded by Cancer
173 Research UK (C14303/A17197, C47594/A16267), the EPSRC-CRUK Cancer Imaging Centre
174 in Cambridge and Manchester (C197/A16465) and the European Union's Seventh Framework
175 Programme (FP7-PEOPLE-2013-CIG-630729).

176 We thank Ewa Klimont and Swapan Preet for α -synuclein protein expression.

177 We thank Jane Gray and Ian Hall from the research instrument core facility of the Cancer
178 Research UK Cambridge Institute for technical support.

179 **Keywords:** Fluorophores • Protein aggregation • Single-molecule imaging • Thioflavin T •
180 Super-resolution • amyloid

181 **Conflicts of interest**

182 There are no conflicts to declare

183 **References**

- 184 1 F. Chiti and C. M. Dobson, *Annu. Rev. Biochem.*, 2017, **86**, 27–68.
- 185 2 V. Kumar, N. Sami, T. Kashav, A. Islam, F. Ahmad and M. I. Hassan, *Eur. J. Med.*
186 *Chem.*, 2016, **124**, 1105–1120.

- 187 3 S. W. Chen, S. Drakulic, E. Deas, M. Ouberai, F. A. Aprile, R. Arranz, S. Ness, C.
188 Roodveldt, T. Williams, E. J. De-Genst, D. Klenerman, N. W. Wood, T. P. J.
189 Knowles, C. Alfonso, G. Rivas, A. Y. Abramov, J. M. Valpuesta, C. M. Dobson and N.
190 Cremades, *Proc. Natl. Acad. Sci.*, 2015, **112**, E1994–E2003.
- 191 4 V. I. Stsiapura, A. A. Maskevich, V. A. Kuzmitsky, V. N. Uversky, I. M. Kuznetsova
192 and K. K. Turoverov, *J. Phys. Chem. B*, 2008, **112**, 15893–15902.
- 193 5 S. Campioni, B. Mannini, M. Zampagni, A. Pensalfini, C. Parrini, E. Evangelisti, A.
194 Relini, M. Stefani, C. M. Dobson, C. Cecchi and F. Chiti, *Nat. Chem. Biol.*, 2010, **6**,
195 140–147.
- 196 6 F. Chiti and C. M. Dobson, *Nat. Chem. Biol.*, 2009, **5**, 15–22.
- 197 7 R. Xing, C. Yuan, S. Li, J. Song, J. Li and X. Yan, *Angew. Chemie Int. Ed.*, 2018, **57**,
198 1537–1542.
- 199 8 D. Hamada, T. Tanaka, G. G. Tartaglia, A. Pawar, M. Vendruscolo, M. Kawamura, A.
200 Tamura, N. Tanaka and C. M. Dobson, *J. Mol. Biol.*, 2009, **386**, 878–890.
- 201 9 N. Cremades, S. I. A. Cohen, E. Deas, A. Y. Abramov, A. Y. Chen, A. Orte, M.
202 Sandal, R. W. Clarke, P. Dunne, F. A. Aprile, C. W. Bertocini, N. W. Wood, T. P. J.
203 Knowles, C. M. Dobson and D. Klenerman, *Cell*, 2012, **149**, 1048–1059.
- 204 10 B. Winner, R. Jappelli, S. K. Maji, P. A. Desplats, L. Boyer, S. Aigner, C. Hetzer, T.
205 Loher, M. Vilar, S. Campioni, C. Tzitzilonis, A. Soragni, S. Jessberger, H. Mira, A.
206 Consiglio, E. Pham, E. Masliah, F. H. Gage and R. Riek, *Proc. Natl. Acad. Sci.*, 2011,
207 **108**, 4194–4199.
- 208 11 S. I. A. Cohen, S. Linse, L. M. Luheshi, E. Hellstrand, D. A. White, L. Rajah, D. E.
209 Otzen, M. Vendruscolo, C. M. Dobson and T. P. J. Knowles, *Proc. Natl. Acad. Sci.*,
210 2013, **110**, 9758–9763.
- 211 12 P. M. Seidler, D. R. Boyer, J. A. Rodriguez, M. R. Sawaya, D. Cascio, K. Murray, T.
212 Gonen and D. S. Eisenberg, *Nat. Chem.*, 2017, **10**, 170–176.
- 213 13 K. Ono, M. M. Condrón and D. B. Teplow, *Structure-neurotoxicity relationships of*
214 *amyloid-protein oligomers*, 2009, vol. 106.
- 215 14 S. L. Shammás, G. A. Garcia, S. Kumar, M. Kjaergaard, M. H. Horrocks, N. Shivji, E.
216 Mandelkow, T. P. J. Knowles, E. Mandelkow and D. Klenerman, *Nat. Commun.*, ,

- 217 DOI:10.1038/ncomms8025.
- 218 15 M. Biancalana, K. Makabe, A. Koide and S. Koide, *J. Mol. Biol.*, 2009, **385**, 1052–
219 1063.
- 220 16 T. Ban, D. Hamada, K. Hasegawall, H. Naiki and Y. Goto, *J. Biol. Chem.*, 2003, **278**,
221 16462–16465.
- 222 17 T. Ban, M. Hoshino, S. Takahashi, D. Hamada, K. Hasegawa, H. Naiki and Y. Goto, *J.*
223 *Mol. Biol.*, 2004, **344**, 757–767.
- 224 18 M. H. Horrocks, S. F. Lee, S. Gandhi, N. K. Magdalinou, S. W. Chen, M. J. Devine, L.
225 Tosatto, M. Kjaergaard, J. S. Beckwith, H. Zetterberg, M. Iljina, N. Cremades, C. M.
226 Dobson, N. W. Wood and D. Klenerman, *ACS Chem. Neurosci.*, 2016, **7**, 399–406.
- 227 19 J. A. Varela, M. Rodrigues, S. De, P. Flagmeier, S. Gandhi, C. M. Dobson, D.
228 Klenerman and S. F. Lee, *Angew. Chemie Int. Ed.*, 2018, **57**, 4886–4890.
- 229 20 N. Amdursky and D. Huppert, *J. Phys. Chem. B*, 2012, **116**, 13389–13395.
- 230 21 M. R. H. Krebs, E. H. C. Bromley and A. M. Donald, *J. Struct. Biol.*, 2005, **149**, 30–37.
- 231 22 M. Iljina, G. A. Garcia, M. H. Horrocks, L. Tosatto, M. L. Choi, K. A. Ganzinger, A. Y.
232 Abramov, S. Gandhi, N. W. Wood, N. Cremades, C. M. Dobson, T. P. J. Knowles and
233 D. Klenerman, *Proc. Natl. Acad. Sci.*, , DOI:10.1073/pnas.1524128113.
- 234 23 K. Spehar, T. Ding, Y. Sun, N. Kedia, J. Lu, G. R. Nahass, M. D. Lew and J.
235 Bieschke, *ChemBioChem*, 2018, 1–6.
- 236 24 N. Banterle, K. H. Bui, E. A. Lemke and M. Beck, 2013, **183**, 363–367.
- 237 25 T. P. J. Knowles, M. Vendruscolo and C. M. Dobson, *Nat. Rev. Mol. Cell Biol.*, 2014,
238 **15**, 384–396.
- 239 26 J. Duboisset, P. Ferrand, W. He, X. Wang, H. Rigneault and S. Brasselet, *J. Phys.*
240 *Chem. B*, , DOI:10.1021/jp309528f.
- 241